34th Annual International Conference of the IEEE EMBS
San Diego, California USA, 28 August - 1 September, 2012

Three-dimensional quantitative ultrasound to guide pathologists towards metastatic foci in lymph nodes

Jonathan Mamou*†, Emi Saegusa-Beecroft‖, Alain Coron‡§, Michael L. Oelze#, Tadashi Yamaguchi<, Junji Machi‖, Masaki Hata‖, Eugene Yanagihara‖, Pascal Laugier‡§, and Ernest J. Feleppa†
†Frederic L. Lizzi Center for Biomedical Engineering, Riverside Research, New York, NY, USA
‖University of Hawaii and Kuakini Medical Center, Honolulu, HI, USA
‡CNRS, UMR 7623, Laboratoire d'Imagerie Paramtrique, F-75006, Paris, France
§UPMC Univ Paris 06, UMR 7623, LIP, F-75005, Paris, France
#Bioacoustics Research Laboratory, University of Illinois at Urbana Champaign, Urbana, IL, USA
<Center for Frontier Medical Engineering, Chiba University, Chiba, Japan
*E-mail: jmamou@riversideresearch.org

***Abstract*—The detection of metastases in freshly-excised lymph nodes from cancer patients during lymphadenectomy is critically important for cancer staging, treatment, and optimal patient management. Currently, conventional histologic methods suffer a high rate of false-negative determinations because pathologists cannot evaluate each excised lymph nodes in its entirety. Therefore, lymph nodes are undersampled and and small but clinically relevant metastatic regions can be missed. In this study, quantitative ultrasound (QUS) methods using high-frequency transducers (i.e., > 20 MHz) were developed and evaluated for their ability to detect and guide pathologists towards suspicious regions in lymph nodes. A custom laboratory scanning system was used to acquire radio-frequency (RF) data in 3D from excised lymph nodes using a 26-MHz center-frequency transducer. Overlapping 1-mm cylindrical regions-of-interest (ROIs) of the RF data were processed to yield 13 QUS estimates quantifying tissue microstructure and organization. These QUS methods were applied to more than 260 nodes from more than 160 colorectal-, gastric-, and breast-cancer patients. Cancer-detection performance was assessed for individual estimates and linear combinations of estimates. ROC results demonstrated excellent classification. For colorectal- and gastric-cancer nodes, the areas under the ROC curves (AUCs) were greater than 0.95. Slightly poorer results (AUC=0.85) were obtained for breast-cancer nodes. Images based on QUS parameters also permitted localization of cancer foci in some micrometastatic cases.**

I. INTRODUCTION

Reliable ultrasound tissue-characterization methods have been sought after for more than three decades. Several tissue properties have been estimated using raw ultrasound data and investigated as tools to diagnose disease states [1], to monitor tissue response to therapies [2], or more fundamentally, to better understand the intricate relationship between ultrasound scattering and tissue properties [3].

High-frequency ultrasound (HFU, >20 MHz) can be used to quantify tissue properties at the microscopic level with spatial resolutions below 100 μm. In this study, HFU was used to develop novel three-dimensional (3D) quantitative ultrasound (QUS) methods to detect and reliably localize metastatic regions in freshly-excised lymph nodes from cancer patients undergoing a lymphadenectomy. Our group previously described the basis of our innovative 3D QUS methods to characterize lymph-node tissues from cancer patients [4]. Our methods demonstrated a potential to reliably determine the presence or absence of metastatic cancer in lymph nodes. Accurate cancer detection is critical for staging disease and planning its treatment. Since our initial successful QUS studies [4], [5], we have improved our methods by adding five novel QUS parameters, and these methods were applied to a larger number of lymph nodes from colorectal-, gastric- and breast-cancer patients.

In the present study, 13 QUS parameters were estimated and used for classification. Four QUS estimates were obtained by quantifying spectrum deduced from the backscattered radio-frequency (RF) echo signals [3], [4], [6] and four QUS estimates were obtained by quantifying the statistics of the envelope-detected echo signals. Specifically, these four envelope parameters were obtained by using the Nakagami and the more-complex homodyned-K (HK) distributions [5]. Finally, the remaining five QUS estimates are also envelope-based but do not rely on a specific model; instead they elegantly quantify the difference between the actual envelope statistics and Rayleigh statistics. The envelope-based QUS estimates are derived from fit parameters associated with the envelope; they hypothetically provide an additional means of distinguishing among tissue types, and they complement the spectral-based QUS estimates [7].

Finally, QUS estimates were used to generate 3D cancer likelihood maps and to visualize the entire lymph node using an interactive 3D display. Such a display could efficiently guide pathologists towards suspicious regions in excised lymph nodes.

This research was supported by NIH Grant CA100183, the Riverside Research Fund for Biomedical Engineering Research, and CNRS.

II. METHODS

A. Surgery and ultrasound data acquisition

Patients with histologically proven colorectal, stomach, or breast cancers were recruited at the Kuakini Medical Center (KMC) in Honolulu, HI. Lymphadenectomy was performed, and several lymph nodes were isolated and sent to the pathology laboratory at KMC. The lymph nodes were grossly prepared for histology and immersed in an isotonic saline (0.9% sodium chloride) bath at room temperature. Individual lymph nodes were scanned in 3D using a single-element spherically-focused transducer (PI30, Olympus NDT, Waltham, MA) having an aperture of 6.1 mm and a focal length of 12.2 mm. The transducer had a center frequency of 25.6 MHz and a -6 dB fractional bandwidth of 67%. The ultrasound RF echo signals were digitized with a sampling frequency of 400 MHz and 8-bit accuracy. Adjacent planes and RF lines were 25 μm apart to cover the entire node in 3D with sufficient spatial sampling.

B. Histology

Following 3D ultrasound scanning, each lymph node underwent non-standard histology processing: the node was inked to recover orientation, cut in half, embedded in a cassette, fixed, sectioned at 65 μm intervals, stained with H&E, and digital images of the slides were obtained with a high-quality high-throughput slide scanner (NanoZoomer, Hamamatsu, Japan) with a pixel resolution of 0.46 μm or with a digital camera (FujiFilm FinePix S9100; Fuji Photo Film, Tokyo, Japan) equipped with Hoya 12 and 14 close-up lenses (Hoya Corp., Tokyo, Japan). Metastatic regions were highlighted in each digital image using custom software. Following digitization, a 3D histology volume was reconstructed from the adjacent images and co-registered with the 3D ultrasound data using the visible ink on the edges of the tissue.

C. QUS estimation

The first processing step was the 3D segmentation of the ultrasound data. Specifically, a semiautomatic 3D segmentation algorithm was implemented to separate lymph-node tissue from surrounding fibroadipose tissue and saline [8]. The segmentation algorithm was based on the watershed transform which yielded many regions within the lymph node. Each region was classified as fibroadipose tissue, saline, or nodal tissue by computing several parameters within each region while taking into account the ultrasound diffraction and attenuation properties, and by using a maximum-likelihood classifier [8]. When necessary, the 3D segmentation was manually corrected using a 3D visualization software that permitted changing the class of each region. Following 3D segmentation, overlapping 3D cylindrical regions-of-interest (ROIs) having a diameter of 1 mm and a length (i.e., measured along the axis of the transducer) of 1 mm [4] were used to yield 13 QUS estimates. These estimates were computed only for ROIs composed entirely of lymph-node tissue as determined by the segmentation algorithm. The methods to estimate the four QUS parameters based on the backscattered signal spectrum and the four QUS parameters based on the Nakagami and homodyned-K distribution for each 3D ROI have been described previously and have not been modified [4], [5].

Five additional envelope-based QUS parameters were computed using a modified quantile-quantile (MQQ) probability plot. Conventional QQ plots are typically used to visually compare two probability density functions (PDFs). In this study, the MQQ plot was used to compare and quantify the estimated PDF of each ROI to that of a Rayleigh PDF. In particular, the MQQ plot was designed such that the MQQ plot of a Rayleigh-distributed ROI would exactly be a straight line with a slope of two. The MQQ plots were parameterized and yielded five QUS estimates quantifying the difference between the ROI PDF and the Rayleigh PDF. A Rayleigh PDF is expected for fully developed speckle in a random medium with randomly-located scatterers [7]. The MQQ-based estimation algorithm was previously used to quantify liver fibrosis [9]. The MQQ-based QUS estimates can be related to tissue microstructure because of their relationship to the well-understood Rayleigh distribution.

D. Classification

A set of uniform lymph nodes (i.e., either entirely devoid of metastatic tissue or completely filled by metastatic tissue) was used to train the classifier. Specifically, the average values of all 13 QUS parameters for each lymph node of the training set were computed, and a linear-discriminant function, D, was computed.

$$D = \sum_{i=1}^{13} \alpha_i E_i = \vec{\alpha} \cdot \vec{E}, \tag{1}$$

where $\vec{\alpha}$ is the vector of linear coefficients and $\vec{E}$ is the vector formed by the 13 QUS estimates. The linear coefficient vector was obtained using the Fisher linear discriminant approach, which maximizes the ratio of the interclass variance to intraclass variance:

$$\vec{\alpha} = (\Sigma_1 + \Sigma_0)^{-1}(\vec{\mu}_1 - \vec{\mu}_0), \tag{2}$$

where Σ_1 and Σ_0 are the covariance matrices of $\vec{E}$ for cancerous and non-cancerous lymph nodes, and $\vec{\mu}_1$ and $\vec{\mu}_0$ are the mean of $\vec{E}$ for cancerous and non-cancerous lymph nodes, respectively. To limit the risk of over classification, a step-wise approach was used to force some of the coordinates of α to be zero if they did not significantly contribute to enhancing the classification.

Classification performance was evaluated by estimating ROC curves and computing the area under the curve (AUC) for each individual QUS estimate and for the optimal linear combination obtained using the step-wise linear-discriminant approach.

Finally, D was used to compute *a posteriori* cancer likelihood for each ROI of each lymph node:

$$P(d) = \frac{e^{-(d-D_1)^2/\sigma_D^2}}{e^{-(d-D_1)^2/\sigma_D^2} + e^{-(d-D_0)^2/\sigma_D^2}}, \qquad (3)$$

where D_1 and D_0 are the mean of the discriminant score for cancerous and non-cancerous nodes, σ_D is the total variance over the training set, and d is the discriminant score for the ROI for which we are computing the cancer likelihood.

III. RESULTS

A. Three-dimensional QUS parametric images

Parametric images depicting effective scatterer sizes are shown in Figs. 1 and 2. Three panels in Fig. 1 show the ultrasound data while the fourth displays the co-registered histology. On the ultrasound panels, segmentation results are shown by the green and red outlines that demarcate the fibroadipose and nodal tissue, respectively. Additionally, the estimated effective scatterer size for each ROI is color-coded and overlaid on the conventional B-mode data. (Figure 2 displays only one cross-sectional ultrasound image and the corresponding histology image.)

The lymph node shown in Fig. 1 was obtained from a colon-cancer patient and did not contain any metastatic foci. The lymph node shown in Fig. 2 was obtained from a different colon-cancer patient and was entirely metastatic. To permit comparison, the color scale for the effective scatterer-size estimates is the same on the two figures. Specifically, the average scatterer-size estimate was 21.3 $\pm$ 1.6 μm for the non-metastatic node and 38.9 $\pm$ 3.0 μm for the metastatic node. These illustrative results suggest that larger scatterer size may reliably indicate metastatic regions within lymph nodes of colon-cancer patients.

B. Classification performance

In total, more than 260 uniform lymph nodes from more than 160 patients were entirely processed and used to train linear-discriminant-based (LDB) classifiers. Table I presents the classification performance results. For each organ, the first line shows the classification results obtained using the single best QUS estimate and the second line shows the results obtained by linearly combining the four QUS estimates. Finally, the last two columns display sensitivity and specificity values obtained at a specific operating point. This operating point was chosen to be clinically conservative (i.e., high sensitivity to limit false-negative determinations at the expense of moderately higher false-positive determinations).

The colorectal-cancer results are very satisfactory and excellent classification performance was obtained with an AUC value of 0.958 using D alone. Note that linear-discriminant analysis did not increase the classification performance. The gastric-cancer results are similar and equally satisfactory when the thirteen QUS estimates were combined, although because of the limited number of cases, greater uncertainty exists. In previous reports, the gastric-cancer nodes were

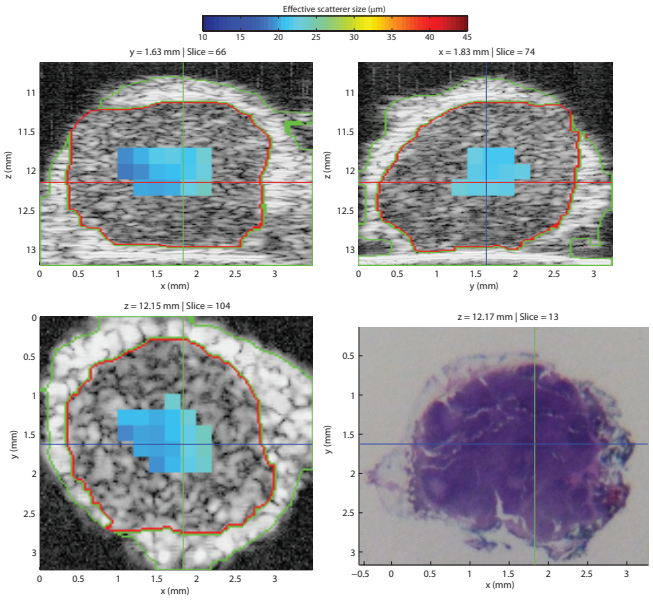

Fig. 1. Three-dimensional cross-sectional parametric images of a non-metastatic lymph node from a colon-cancer patient. Effective scatterer-size estimates are color-coded and overlaid on the three conventional B-mode images. Co-registered histology is also shown.

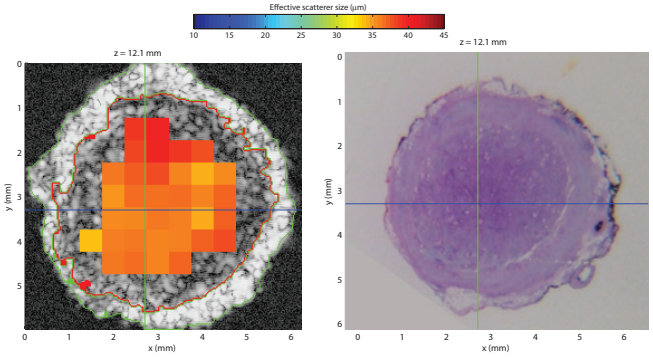

Fig. 2. Cross-sectional parametric images of an entirely-metastatic lymph node from a colon-cancer patient. Effective scatterer-size estimates are color-coded and overlaid on the conventional B-mode images. Co-registered histology is also shown.

analyzed in combination with the colorectal nodes because their histologic differences are minute [5] and because the number of cases previously was insufficient for independent analysis.

The breast-cancer nodes are structurally very different from the gastric- and colorectal-cancer nodes, and classification performance was poorer with an AUC of 0.847 using linear-discriminant analysis. Note that the single best QUS estimates (i.e., MQQ estimate S_a) led to very poor classification with an AUC value of only 0.727. These results might indicate that the scattering models used are not well adapted to lymph nodes obtained from breast-cancer patients.

Finally, the sensitivity and specificity values quoted in

TABLE I
CLASSIFICATION PERFORMANCE OF QUS. AREAS UNDER THE ROC CURVE (AUC)

Primary Organ	Patient number	Total nodes	Cancer nodes	Non-cancer nodes	Parameter	ROC AUC	Sensitivity	Specificity
Colorectal	77	140	21	119	D	0.958±0.012	90.5%	85.7%
					LDB	0.958±0.012	90.5%	85.7%
Gastric	17	25	5	20	D	0.880±0.069	100%	85.0%
					LDB	0.950±0.044	100%	90.0%
Breast	74	102	16	86	S_a	0.727 ±0.066	93.8%	32.6%
					LDB	0.847 ±0.053	93.8%	55.8%

Table I clearly indicate that the QUS methods are reliable and could drastically reduce the number of false-negative determinations. (False-positive determinations very rarely occur in the current standard of care using histology.)

C. Three-dimensional cancer likelihood images

The classifiers obtained from the uniform nodes were applied to our entire lymph-node database, in particular, to partially metastatic lymph nodes. Discriminant scores were converted to cancer-likelihood values; and 3D cancer-likelihood maps were generated and compared to co-registered histology. Figure 3 displays an illustrative image of a partially-metastatic axillary lymph node obtained from a breast-cancer patient. This image in analogous to Figure 1 except that regions in the lymph node having a QUS-derived cancer likelihood greater than 50% are highlighted in red and that in the histology image (bottom right panel), the metastatic regions were outlined in green by the pathologist. Figure 3 indicates that the metastatic foci were well detected in the B-mode images augmented with cancer the likelihood overlay.

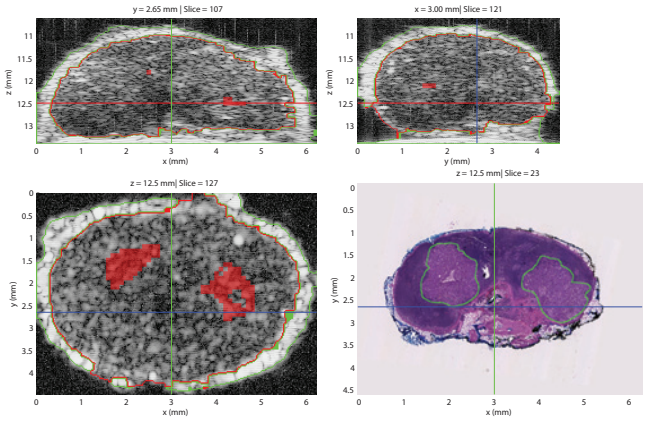

Fig. 3. Three-dimensional cross-sectional parametric images of a partially metastatic lymph node from a breast-cancer patient. Red highlights symbolize cancer likelihood greater than 50%. Co-registered histology photo micrograph showing metastatic regions in green is also shown.

IV. CONCLUSIONS

This study establishes the potential strength of QUS-based detection of metastases regions in dissected lymph nodes. These QUS methods were able to yield high sensitivity while maintaining satisfactory specificity. Therefore, the results to date suggest that these methods have great potential for specific detection and localization of micrometastases often missed during conventional histology. Finally, the 3D cancer-likelihood maps could serve as basis for the development of a novel pathology tool. A low-cost and small-footprint device could be designed to quickly scan lymph nodes, obtain QUS estimates, and guide the pathologist towards suspicious regions. Such a tool could be invaluable for reducing the current rate of false-negative determinations.

REFERENCES

[1] E. J. Feleppa, J. Mamou, C. R. Porter, and J. Machi, "Quantitative ultrasound in cancer imaging," *Semin Oncol*, vol. 38, no. 1, pp. 136–50, 2011.

[2] R. M. Vlad, S. Brand, A. Giles, M. C. Kolios, and G. J. Czarnota, "Quantitative ultrasound characterization of responses to radiotherapy in cancer mouse models," *Clin Cancer Res*, vol. 15, no. 6, pp. 2067–75, 2009.

[3] F. L. Lizzi, M. Greenebaum, E. J. Feleppa, M. Elbaum, and D. J. Coleman, "Theoretical framework for spectrum analysis in ultrasonic tissue characterization," *J. Acoust. Soc. Am.*, vol. 73, pp. 1366–1373, April 1983.

[4] J. Mamou, A. Coron, M. Hata, J. Machi, E. Yanagihara, P. Laugier, and E. J. Feleppa, "Three-dimensional high-frequency characterization of cancerous lymph nodes," *Ultrasound Med Biol*, vol. 36, pp. 361–375, 2010.

[5] J. Mamou, A. Coron, M. L. Oelze, E. Saegusa-Beecroft, M. Hata, P. Lee, J. Machi, E. Yanagihara, P. Laugier, and E. J. Feleppa, "Three-dimensional high-frequency backscatter and envelope quantification of cancerous human lymph nodes," *Ultrasound Med Biol*, vol. 37, no. 3, pp. 345–57, 2011.

[6] M. F. Insana, R. F. Wagner, D. G. Brown, and T. J. Hall, "Describing small-scale structure in random media using pulse-echo ultrasound," *J. Acoust. Soc. Am.*, vol. 87, pp. 179–192, 1990.

[7] R. F. Wagner, M. F. Insana, and D. G. Brown, "Statistical properties of radio-frequency and envelope-detected signals with applications to medical ultrasound," *J Opt Soc Am A*, vol. 4, no. 5, pp. 910–922, 1987.

[8] A. Coron, J. Mamou, M. Hata, J. Machi, E. Yanagihara, P. Laugier, and E. J. Feleppa, "Three-dimensional segmentation of high-frequency ultrasound echo signals from dissected lymph nodes," *Proceedings of the 2008 IEEE Ultrasonics Symposium*, pp. 1370–1373, 2008.

[9] T. Yamaguchi and H. Hachiya, "Proposal of a parametric imaging method for quantitative diagnosis of liver fibrosis," *J Med Ultrasonics*, vol. 37, pp. 155–166, 2010.